Published in final edited form as:

Curr Biol. 2020 February 24; 30(4): 708–714.e4. doi:10.1016/j.cub.2019.12.021.

Niche cell wrapping ensures primordial germ cell quiescence and protection from intercellular cannibalism

Daniel C. McIntyre[1], **Jeremy Nance**[1,2,3,*]

[1]Skirball Institute of Biomolecular Medicine, NYU School of Medicine, New York, NY 10016

[2]Department of Cell Biology, NYU School of Medicine, New York, NY 10016

[3]Lead Contact

SUMMARY

Niche cells often wrap membrane extensions around stem cell surfaces. Niche wrapping has been proposed to retain stem cells in defined positions and affect signaling [eg. 1, 2]. To test these hypotheses and uncover additional functions of wrapping, we investigated niche wrapping of primordial germ cells (PGCs) in the *C. elegans* embryonic gonad primordium. The gonad primordium contains two PGCs that are wrapped individually by two somatic gonad precursor cells (SGPs). SGPs are known to promote PGC survival during embryogenesis and exit from quiescence after hatching, although how they do so is unknown [3]. Here, we identify two distinct functions of SGP wrapping that are critical for PGC quiescence and survival. First, niche cell wrapping templates a laminin-based basement membrane around the gonad primordium. Laminin and the basement membrane receptor dystroglycan function to maintain niche cell wrapping, which is critical for normal gonad development. We find that laminin also preserves PGC quiescence during embryogenesis. Exit from quiescence following laminin depletion requires *glp-1/Notch* and is accompanied by inappropriate activation of the GLP-1 target *sygl-1* in PGCs. Independent of basement membrane, SGP wrapping performs a second, crucial function to ensure PGC survival. Endodermal cells normally engulf and degrade large lobes extended by the PGCs [4]. When SGPs are absent, we show that endodermal cells can inappropriately engulf and cannibalize the PGC cell body. Our findings demonstrate how niche cell wrapping protects germ cells by manipulating their signaling environment and by shielding germ cells from unwanted cellular interactions that can compromise their survival.

Keywords

Primordial germ cell; stem cell; niche; Notch; wrapping; basement membrane; quiescence; cell death; dystroglycan; laminin

[*]**Correspondence**: Jeremy Nance, NYU School of Medicine, Skirball Institute of Biomolecular Medicine, 540 First Avenue, 4th floor lab 17, New York, NY 10016, 212-263-3156, Jeremy.Nance@med.nyu.edu.

AUTHOR CONTRIBUTIONS

D.C.M. and J.N. designed and conducted experiments, analyzed the data and prepared the manuscript.

DECLARATION OF INTERESTS

The authors have no competing interests to declare.

RESULTS

SGP Wrapping Templates the Gonadal Basement Membrane

SGPs migrate to and wrap around PGCs during the first half of embryogenesis (Figure 1A). A basement membrane (BM) surrounds the gonad primordium as well as other organs, and depletion of several BM components, including laminin, disrupts gonad organization in larvae [5–7]. BM assembles when laminin trimers containing α, β and γ subunits concentrate on cellular surfaces and recruit additional BM components [8]. *lam-1* encodes the sole *C. elegans* laminin ß. Functional LAM-1^{GFP} [9] concentrated on outward-facing SGP surfaces (SGP^{Mem}) soon after SGPs wrapped the PGCs but was not present on SGP surfaces facing the PGCs (Figures 1B and S1A). *C. elegans* expresses two laminin a subunits, EPI-1 and LAM-3, which can function redundantly [5]. Consistent with observations in larvae [5], we detected only EPI-1 in the gonadal BM, whereas both proteins were present in many other BMs (Figures 1C and 1D). Laser-ablating the SGP precursors to block SGP-PGC interactions prevented LAM-1^{GFP} from enriching around the naked PGCs (Figures 1E and S1B), indicating that SGP wrapping of PGCs templates the gonadal BM.

Basement Membrane has Distinct Roles in Initiating and Maintaining SGP Wrapping

To determine the role of the gonadal BM, we examined SGPs and PGCs in laminin-depleted late-stage embryos. Depleting *lam-1* or *lam-2* (the sole *laminin γ*) blocks laminin trimer assembly, disrupts BM formation (Figure S2A), and causes late embryonic arrest [5, 7, 10]. In most *lam-1(RNAi)* and *lam-2(RNAi)* embryos, one or both SGPs were not wrapped around a PGC (Figures 2A and 2B). *epi-1(RNAi)* embryos showed nearly identical phenotypes, whereas *lam-3* mutant embryos had no defects in SGP wrapping (Figures 2A, 2B, S2B and S2C). The distinct phenotypes of *epi-1(RNAi)* and *lam-3* mutant embryos suggest that loss of gonadal BM, which contains EPI-1 but not LAM-3, underlies the SGP wrapping defects of laminin-depleted embryos.

We established when SGP wrapping defects arose by capturing movies of *lam-1(RNAi)* and *lam-2(RNAi)* early embryos as the gonad primordium assembled. Two classes of defects were apparent (Figures 2C and 2D). In Class I embryos, one SGP failed to wrap its PGC (8%). In Class II embryos, an SGP that initially failed to wrap the PGC cell body recovered by a later stage (33%). Because gonadal BM formation requires SGP wrapping, we infer that these wrapping initiation defects result from loss of non-gonadal BM. Additionally, since a considerably larger fraction of late-stage laminin-depleted embryos showed wrapping defects (95%, Figure 2B), we conclude that laminin has roles in both initiating and maintaining SGP wrapping. We propose that non-gonadal BM is required for migratory SGPs to transition to a wrapped state [11], and that gonadal BM, after being assembled by SGPs, ensures that SGP wrapping is maintained. The latter conclusion is supported by the finding that *epi-1(RNAi)* embryos have only minor defects in wrapping initiation (Figure 2D) but defects as severe as those of *lam-1(RNAi)* and *lam-2(RNAi)* embryos in wrapping maintenance (Figure 2B).

The wrapping maintenance defects of laminin-depleted embryos suggest that SGPs utilize a BM receptor to prevent their wrapping membranes from retracting. In larvae, the laminin

receptor DGN-1/dystroglycan is enriched in gonadal BM and is required for gonad organization [6], suggesting that DGN-1 could anchor SGP membranes to the gonadal BM. We detected endogenously tagged DGN-1 (DGN-1^{mNG}) [12] at outward-facing SGP surfaces soon after SGP wrapping was complete (Figures 1F and S1C). Most SGPs in *dgn-1* mutant late-stage embryos failed to maintain wrapping (Figures 2A and 2C), even though *dgn-1* is not required to form the gonadal BM [6] and comparatively fewer *dgn-1* mutant embryos showed wrapping initiation defects (Figure 2D). These findings suggest that DGN-1 is the major BM receptor responsible for maintaining SGP wrapping and also plays a role in wrapping initiation.

Basement Membrane Ensures PGC Quiescence by Inhibiting GLP-1/Notch Signaling

Wild-type embryos always contain two PGCs (Figure 2F), which remain quiescent until the embryo hatches in the presence of food [13]. Unexpectedly, we observed 3-4 PGCs in many *lam-1(RNAi)* and *lam-2(RNAi)* embryos, and confirmed these RNAi results using *lam-1(ok3139)* mutants (Figures 2E and 2F). In movies of *lam-1(RNAi)* embryos, extra PGCs always resulted from a single extra division of one or both PGCs (Figure S3A, 8/8 embryos). *epi-1(RNAi)* embryos but not *lam-3* mutant embryos also contained extra PGCs (Figure 2F), suggesting that gonadal BM is required for PGCs to remain quiescent before embryos hatch and begin feeding. *dgn-1* mutant embryos never contained extra PGCs (Figure 2F), despite the requirement for *dgn-1* in maintaining SGP wrapping, indicating that gonadal BM maintains SGP wrapping and inhibits PGC proliferation through distinct mechanisms.

Loss of *daf-18/pten* causes PGCs in newly hatched larvae to divide even in the absence of food, and this phenotype is suppressed by mutations in its downstream effector *akt-1* [14]. However, *lam-1(RNAi)* and *lam-1(RNAi) akt-1* embryos had equivalent numbers of extra PGCs (Figure S3B), suggesting that the *daf-18* pathway is not responsible for extra PGCs in laminin-depleted embryos. In larvae and adults, GLP-1/Notch is required to maintain germline stem cell identity and number [13], although GLP-1 is not known to regulate embryonic PGCs. We tested whether GLP-1 was required for extra PGCs in laminin-depleted embryos using two temperature-sensitive *glp-1* mutations. Both alleles significantly suppressed the extra PGC phenotype of *lam-1* mutant embryos (Figure 2G). In larvae, GLP-1 promotes germline stem cell maintenance by activating its redundant transcriptional targets *sygl-1* and *lst-1* [15]. A *sygl-1* transcriptional reporter [15], which is not normally expressed in embryonic PGCs (Figure 2I), was significantly upregulated in *lam-1(RNAi)* and *epi-1(RNAi)* embryos (Figures 2I and 2J), and *sygl-1 lst-1* double mutants partially suppressed the PGC proliferation phenotype of *lam-1(RNAi)* and *epi-1(RNAi)* embryos (Figure 2H). Together, these findings suggest that loss of gonadal BM inappropriately activates GLP-1/Notch signaling in PGCs, causing loss of PGC quiescence. Because we did not observe extra PGCs in wild-type or laminin-depleted embryos with ablated SGPs (Table 1), it is likely that activation of GLP-1 in laminin-depleted embryos requires signaling from the SGPs, which are normally in contact with the gonadal BM.

SGPs Promote PGC Survival by Preventing Endodermal Cell Cannibalization

Surprisingly, a small number of laminin-depleted embryos showed the opposite phenotype - too few PGCs (Figures 2E and 2F). Movies of *lam-1(RNAi)* embryos showed that loss of PGCs resulted from PGC death (9/9 embryos, Figure 3A). Dying PGCs transitioned through two distinct stages. Initially, both membrane and nuclear mCherry markers concentrated within the cytoplasm (Figure 3A, 4:00). Subsequently, the dying PGC condensed into compact debris (Figure 3A, 4:50). In contrast to apoptotic corpses, which are refractile when viewed by DIC, dying PGCs did not appear distinct (Figure S4A). PGC death in *lam-1(RNAi)* embryos always correlated with a complete failure of SGP wrapping (Class I phenotype, Figure 2D) when the gonad first forms (9/9 embryos), suggesting that PGC death is normally prevented by SGP wrapping. We conclude that laminin promotes PGC survival, independently of its later role in maintaining gonad integrity, by enabling SGP wrapping when the gonad primordium assembles.

To directly test whether SGPs are required for PGC survival, we laser-ablated the SGP precursors. Using DIC microscopy, Kimble and White [3] reported that PGCs were missing in SGP-ablated embryos but did not determine when or how they disappeared. We found that one or both PGCs were frequently absent when SGP-ablated embryos hatched (40% lost), in contrast to control-ablated embryos (Table 1 and Figure S4A). Approximately half as many PGCs (17%) were lost in embryos with one ablated SGP precursor, and the surviving PGC invariably contacted the un-ablated SGP (Table 1 and Figure S4A). We confirmed these findings using a genetic approach by examining *ehn-3 hnd-1(RNAi)* L1 larvae, which specifically lack SGPs [16] (Table 1). In contrast to apoptotic cell death, which requires *ced-3/caspase* [17], *ced-3* was not required for PGC death in embryos lacking SGPs (Table 1). These findings strongly suggest that contact with an SGP prevents PGC death through a non-apoptotic mechanism. Depleting laminin did not enhance the PGC death seen when SGP precursors were ablated (Table 1), further supporting the conclusion that laminin prevents PGC death by ensuring that SGPs are able to find and wrap PGCs.

As the gonad primordium forms, PGCs form large lobes that are cannibalized and digested in late-stage embryos by endodermal cells [4]. We observed that compact debris from dead PGCs in SGP-ablated embryos was always present inside of endodermal cells (8/8 embryos), and in some embryos we observed a PGC cell body within an endodermal cell (4/16 embryos, Figure 3B), suggesting that SGP wrapping might prevent endodermal cells from cannibalizing the PGC cell body. Supporting this idea, in SGP-ablated embryos PGCs were often positioned abnormally (Figures 3C and 3D), and their cell body frequently contacted endodermal cells (Figures S4B and S4C). These defects were present at early stages when the gonad primordium normally forms.

To test if endodermal cells are necessary for PGC death, we examined endoderm-less *end-1 end-3* mutants [18]. Most *end-1 end-3* embryos contained two SGPs that contacted the PGCs, even though PGC position was often aberrant [19]. Remarkably, in *end-1 end-3* mutants lacking SGPs, only 3% of PGCs died (Table 1 and Figure 3E), in contrast to control SGP-ablated embryos (rescued *end-1 end-3* mutants), in which 53% of PGCs died (Table 1). These findings indicate that in the absence of SGPs, PGCs die when they are cannibalized by endodermal cells.

Endodermal cells assemble a scission complex of F-actin and dynamin to cut off PGC lobes, and scission complex formation requires CED-10/Rac and LST-4/SNX9 [4]. To determine whether a scission step is needed for endodermal cells to cannibalize the PGC cell body, we ablated SGP precursors in *ced-10* and *lst-4* mutant embryos, in which most PGC lobes persist [4]. PGCs rarely died in *ced-10* and *lst-4* mutants lacking SGPs (Table 1), and we detected PGC cell bodies surrounded by endodermal cells connected to external, unengulfed lobes (Figures 3F and 3G; *ced-10*, 5/15 embryos). We conclude that SGPs normally prevent endodermal cells from engulfing, severing, and digesting the PGC cell body.

DISCUSSION

Our findings show that formation of the *C. elegans* PGC niche is a multi-step developmental process involving initial wrapping by niche (SGP) cells, local assembly of basement membrane on niche cell membranes, and dystroglycan-mediated adhesion to gonadal BM that anchors niche cell wrapping membranes in place. PGCs may play an active role in promoting wrapping, as their descendants have been described to do in larvae [20]. Although the function of wrapping by niche cells is poorly understood, previous studies have suggested that wrapping regulates stem cell behavior by modulating the local signaling environment [2, 21, 22]. We showed that SGP wrapping influences PGC signaling by establishing a gonadal BM, which maintains PGC quiescence by inhibiting GLP-1/Notch activity. While it is not yet apparent how gonadal BM inhibits Notch signaling, BM could influence the availability of Notch ligands or regulators, similar to the role of collagen in locally enriching the Notch regulator BMP to promote *Drosophila* intestinal stem cell self-renewal [23]. These findings raise the intriguing possibility that changes in gonadal BM structure or composition after hatching might be needed to promote GLP-1/Notch signaling in larval germ cells. As Notch is required for the maintenance of many types of stem cells [eg. 24, 25], its regulation by niche BM might provide an underappreciated yet critical signaling input.

We uncovered an additional, unexpected function for niche cell wrapping – providing physical protection to stem cells from potentially lethal interactions with neighboring cells – in this case cannibalism of PGCs by endodermal cells. We propose that the initial wrapping of the PGC cell body by SGPs ensures that endodermal cells only have access to the PGC lobes, which they subsequently consume [4]. This role of SGP wrapping is most likely independent of the gonadal BM since SGPs are required to prevent inappropriate contact between the PGC cell body and endodermal cells at the earliest stages of gonad primordium formation, before the gonadal BM is apparent; because PGCs in laminin-depleted embryos never die if they are initially wrapped successfully by an SGP; and since a far-greater percentage of PGCs die in SGP-ablated embryos than in *lam-1* mutant embryos. Collectively, our findings reveal the critical importance of niche cell wrapping in creating a BM that regulates germ cell quiescence, and in protecting germ cells from cellular interactions that can compromise their survival.

STAR METHODS

LEAD CONTACT AND MATERIALS AVAILABILITY

Further information and requests for resources and reagents should be directed to and will be fulfilled by the Lead Contact, Jeremy Nance, Jeremy.Nance@med.nyu.edu. All materials described in this manuscript are either commercially available or available from the authors upon request. Raw data are available upon request.

EXPERIMENTAL MODEL AND SUBJECT DETAILS

Worm Strains—Worms were cultured under standard conditions at room temperature [26] except for *glp-1* temperature sensitive mutants, which were maintained at 20°C. To block *glp-1* function in the gonad primordium, *glp-1 (ts)* embryos were shifted to 25.5°C after the 128-cell stage in order to bypass required GLP-1 functions during the first few cleavage cycles of embryogenesis. Strain N2 (Bristol) was used as wild type. Strains utilized in this study are listed in detail in the Key Resources Table. The *akt-1(ok525)* allele is a 1251bp deletion that removes the kinase domain and is predicted to be a null.

METHOD DETAILS

Transgene construction

***ehp-3p::mCherry-PH$_{PLC1\partial1}$* (pYA12):** PCR was used to construct Gateway (Invitrogen) entry vectors for the *ehn-3* promoter up to the second exon (5' entry clone; base pairs −2751 to +323 of *ehn-3)* and mCherry-PH$_{PLC1\partial1}$ (middle entry clone, amplified from *end-1p::mCherry-PH$_{PLC1\partial1}$* [19]). Together with the *tbb-2* 3' UTR 3' entry clone [27], entry clones were recombined with destination vector pCFJ150 [28] using MultiSite Gateway (Invitrogen). The pCFJ150 destination vector contains *C. briggsae unc-119(+)* for use as a transformation marker.

***ehp-3p::YFP* (pDCM03):** The *mCherry-PH$_{PLC1\partial1}$* in pYA12 was replaced by *YFP* amplified from pPD134.99 (Fire Lab *C. elegans* Vector Kit, Addgene kit #1000000001) using Gibson Assembly [29].

***end-1p::CFP-CAAX* (pJN585).:** *GFP* in plasmid *end-1p::GFP-CAAX* [30] was replaced with *CFP* amplified from plasmid pPD134.96 (Fire Lab *C. elegans* Vector Kit, Addgene kit #1000000001) using Gibson Assembly[29].

Worm transformation—Plasmids were injected into *unc-119(ed3)* worms (*end-1p::CFP-CAAX* was injected together with *C. elegans unc-119(+)* plasmid pJN254 [31]) to obtain extrachromosomal arrays [32]. *ehn-3p::mCherry-PH$_{PLC1\partial1}$* and *ehn-3p::YFP* extrachromosomal arrays were integrated using Trioxsalen (Sigma, T6137) and UV irradiation, as described [33].

RNAi—L4 larvae were fed *E. coli* bacterial strain HT115 expressing dsRNA from plasmid pPD129.36 (control) or derivatives containing sequences targeting specific genes. Worms were fed for two days at 23°C before progeny were collected for analysis. For all RNAi experiments, negative control embryos were from worms fed empty pPD129.36 vector. All

results presented include pooled data from at least three independent trials. RNAi feeding plasmid targeting *epi-1* was obtained from the Ahringer RNAi library (clone K08C7.3) [34]. All other RNAi feeding plasmids were constructed from PCR-amplified cDNA ligated into pPD129.36 vector using Gibson Assembly and the following primers:

lam-1: 5'–GTGCCGACATTACTCATTACG–3', 5'–CTCCGAGTCTTGGATCTC–3'

lam-2: 5'–CCCAAGAATCAATGAACTCGAA-3', 5'–CATCCATTGGCACTGAATCC–3'

hnd-1: 5'–CTGGAAACAATGCGGTTTCT-3', 5'–CCGGAAACGGACTTTACAAT–3'

The effectiveness of laminin subunit RNAi was confirmed by assaying LAM-1^{GFP} expression, which was absent in *lam-1 (RNAi)* embryos, and absent from gonadal basement membranes in *lam-2(RNAi)* and *epi-1(RNAi)* embryos (Figure S2). *hnd-1* RNAi effectiveness was confirmed by the loss of SGP marker *ehn-3p::YFP* in the *ehn-3(q689)* genetic background (Table 1).

SGP laser ablation—Cells were ablated using a MicroPoint tunable laser (Oxford Instruments) with a 440 nm Coumarin dye cell installed on a Zeiss AxioImager and observed using a 100X 1.3NA objective lens. Embryos were mounted on a 3% agarose pad under a #1.5 coverslip. Nuclei in targeted cells were ablated with 10-15 laser pulses, until refractile debris was evident in the nucleus. Ablation of the SGP precursors was verified using DIC imaging or, in most experiments, by the failure of embryos to express the SGP-specific *ehn-3p::YFP* transgene. Ablated cells ceased dividing and were not engulfed by other cells during the course of the experiments. To eliminate both SGPs, the MSapp and MSppp blastomeres were targeted. Control unablated embryos were mounted on the same slides as experimental embryos and allowed to develop simultaneously. In control ablated embryos, the sisters of MSapp and MSppp were targeted (MSapa and MSppa). These embryos always contained two SGPs and two PGCs (15/15). In some cases, laser ablation caused damage to nearby control unablated embryos, which were mounted on the same slide. These experiments were discarded and repeated.

Immunostaining—Embryos were collected from rinsed gravid hermaphrodites that were incubated in water for 4 hours to allow eggs to age. Fixation and immunostaining were performed as described [35] using the following primary and secondary antibodies: chicken anti-EPI-1 (1:8) [5], chicken anti-LAM-3 (1:8) [5], mouse anti-FRM-1 (1:1000) [36], Alexa Fluor 647 donkey anti-chicken IgY (1:500, Jackson ImmunoResearch), and Alexa Fluor 488 goat anti-mouse IgG (1:1000, Invitrogen).

Microscopy—Images of fixed embryos and time-lapse movies were acquired on a Zeiss AxioImager.A2 equipped with an AxioCam 503 mono CCD camera, Uniblitz shutter, and 63X 1.4NA or 40X 1.3NA objective. Images of SGPs and PGCs in SGP ablation experiments at bean stage and 1.5-fold stage were acquired on a Leica SP5 II confocal microscope with a 63X 1.4NA objective. For live imaging, embryos were mounted on 3% agarose pads in Egg Salts buffer. L1 larva were immobilized by adding 1.5ul of 5mM levamisole to the coverslip before it was placed over the agarose pad. Three-fold embryos

were immobilized using a custom-built gas exchange slide pressurized with nitrogen (3-5 PSI). The top of the chamber contains a #1.5 coverslip; embryos were placed on the inside of the coverslip, sandwiched under a 3% agarose pad. After ~10 minutes in nitrogen, embryos ceased moving, but resumed movement and completed development once the chamber was vented with room air. Unless otherwise specified, Z-stacks were spaced at 500nm. For time-lapse imaging, Z-stacks were acquired every 25 to 30 minutes as indicated. Image stacks were deconvolved using Zeiss Zen software, and processed in ImageJ and Adobe Photoshop.

QUANTIFICATION AND STATISTICAL ANALYSIS

Laminin intensity measurements—To measure LAM-1^{GFP} intensity after SGP ablation, equal exposure times were used to capture images in control and SGP-ablated embryos, background fluorescence was subtracted using ImageJ, and maximum pixel intensity (averaged over a line 10 pixels in width) was measured across the gonadal BM on the side of the PGCs facing the endoderm and compared as a ratio with the same measurement across an unaffected reference BM (along the ventral side of the endoderm).

PGC nucleus position—To measure the position of PGC nuclei within the embryo, the following two measurements were made: 1) using ImageJ, the center of each nucleus was marked and its distance to the midline of the embryo was calculated by drawing the shortest possible line between that point and the midline; 2) using ImageJ, the center of each nucleus was marked and its distance to the anterior end of the embryo was calculated by drawing the shortest possible line between that point and a tangential line orthogonal to the anterior end of the eggshell. This distance was then normalized to the total length of the egg.

***sygl-1*::H2B-GFP intensity measurements—**To measure H2B-GFP intensity in PGCs, equal exposure settings were used to capture images from embryos treated with each type of RNAi, total pixel intensity was measured in a 4μm diameter circle containing the PGC nucleus, and background fluorescence was subtracted by measuring GFP intensity in a region of the same size outside of the PGC.

Statistics and reproducibility—Data sets presented include at least three independent experiments and the minimum sample size relied upon was ten unless indicated otherwise. Power calculations were not used to determine sample sizes, and experiments were not randomized nor blinded before analysis. During data collection, damaged embryos were excluded from analysis. Statistical tests used are indicated in figure legends and table footnotes. In cases where multiple comparisons were made, *p*-values were corrected using the Bonferroni method. For *t*-test comparisons between two or more samples, data normality was assessed using the Shapiro-Wilk normality test.

DATA CODE AND AVAILABILITY

This study did not generate any datasets or code.

Supplementary Material

Refer to Web version on PubMed Central for supplementary material.

ACKNOWLEDGMENTS

We thank David Sherwood for reagents, and Erika Bach, Jane Hubbard, and Prash Rangan for comments on the manuscript. Some strains were provided by the CGC, which is funded by NIH Office of Research Infrastructure Programs (P40 OD010440). Funds were provided to J.N. by NYSTEM (C029561) and the NIH (R21HD084809 and R35GM118081), and to D.C.M. from the American Cancer Society Eastern Division (New York Cancer Research Fund Postdoctoral Fellowship, PF-16-098-01-DDC).

REFERENCES

1. Tamplin OJ, Durand EM, Carr LA, Childs SJ, Hagedorn EJ, Li P, Yzaguirre AD, Speck NA, and Zon LI (2015). Hematopoietic stem cell arrival triggers dynamic remodeling of the perivascular niche. Cell 160, 241–252. [PubMed: 25594182]
2. Byrd DT, Knobel K, Affeldt K, Crittenden SL, and Kimble J (2014). A DTC niche plexus surrounds the germline stem cell pool in *Caenorhabditis elegans*. PLoS One 9, e88372. [PubMed: 24586318]
3. Kimble JE, and White JG (1981). On the control of germ cell development in *Caenorhabditis elegans*. Dev Biol 81, 208–219. [PubMed: 7202837]
4. Abdu Y, Maniscalco C, Heddleston JM, Chew TL, and Nance J (2016). Developmentally programmed germ cell remodelling by endodermal cell cannibalism. Nat Cell Biol 18, 1302–1310. [PubMed: 27842058]
5. Huang CC, Hall DH, Hedgecock EM, Kao G, Karantza V, Vogel BE, Hutter H, Chisholm AD, Yurchenco PD, and Wadsworth WG (2003). Laminin alpha subunits and their role in *C. elegans* development. Development 130, 3343–3358. [PubMed: 12783803]
6. Johnson RP, Kang SH, and Kramer JM (2006). *C. elegans* dystroglycan DGN-1 functions in epithelia and neurons, but not muscle, and independently of dystrophin. Development 133, 1911–1921. [PubMed: 16611689]
7. Kao G, Huang CC, Hedgecock EM, Hall DH, and Wadsworth WG (2006). The role of the laminin beta subunit in laminin heterotrimer assembly and basement membrane function and development in *C. elegans*. Dev Biol 290, 211–219. [PubMed: 16376872]
8. Yurchenco PD (2015). Integrating Activities of Laminins that Drive Basement Membrane Assembly and Function. Curr Top Membr 76, 1–30. [PubMed: 26610910]
9. Ziel JW, Hagedorn EJ, Audhya A, and Sherwood DR (2009). UNC-6 (netrin) orients the invasive membrane of the anchor cell in *C. elegans*. Nat Cell Biol 11, 183–189. [PubMed: 19098902]
10. Rasmussen JP, Reddy SS, and Priess JR (2012). Laminin is required to orient epithelial polarity in the *C. elegans* pharynx. Development 139, 2050–2060. [PubMed: 22535412]
11. Rohrschneider MR, and Nance J (2013). The union of somatic gonad precursors and primordial germ cells during *Caenorhabditis elegans* embryogenesis. Dev Biol 379, 139–151. [PubMed: 23562590]
12. Naegeli KM, Hastie E, Garde A, Wang Z, Keeley DP, Gordon KL, Pani AM, Kelley LC, Morrissey MA, Chi Q, et al. (2017). Cell Invasion In Vivo via Rapid Exocytosis of a Transient Lysosome-Derived Membrane Domain. Dev Cell 43, 403–417 e410. [PubMed: 29161591]
13. Kimble J, and Crittenden SL (2005). Germline proliferation and its control. WormBook, 1–14.
14. Fukuyama M, Rougvie AE, and Rothman JH (2006). *C. elegans* DAF-18/PTEN mediates nutrient-dependent arrest of cell cycle and growth in the germline. Curr Biol 16, 773–779. [PubMed: 16631584]
15. Kershner AM, Shin H, Hansen TJ, and Kimble J (2014). Discovery of two GLP-1/Notch target genes that account for the role of GLP-1/Notch signaling in stem cell maintenance. Proc Natl Acad Sci U S A 111, 3739–3744. [PubMed: 24567412]
16. Mathies LD, Henderson ST, and Kimble J (2003). The *C. elegans* Hand gene controls embryogenesis and early gonadogenesis. Development 130, 2881–2892. [PubMed: 12756172]

17. Ellis HM, and Horvitz HR (1986). Genetic control of programmed cell death in the nematode *C. elegans*. Cell 44, 817–829. [PubMed: 3955651]

18. Owraghi M, Broitman-Maduro G, Luu T, Roberson H, and Maduro MF (2010). Roles of the Wnt effector POP-1/TCF in the *C. elegans* endomesoderm specification gene network. Dev Biol 340, 209–221. [PubMed: 19818340]

19. Chihara D, and Nance J (2012). An E-cadherin-mediated hitchhiking mechanism for *C. elegans* germ cell internalization during gastrulation. Development 139, 2547–2556. [PubMed: 22675206]

20. Gordon KL, Payne SG, Linden-High LM, Pani AM, Goldstein B, Hubbard EJA, and Sherwood DR (2019). Ectopic Germ Cells Can Induce Niche-like Enwrapment by Neighboring Body Wall Muscle. Curr Biol 29, 823–833 e825. [PubMed: 30799241]

21. Buszczak M, Inaba M, and Yamashita YM (2016). Signaling by Cellular Protrusions: Keeping the Conversation Private. Trends Cell Biol 26, 526–534. [PubMed: 27032616]

22. Chen S, Lewallen M, and Xie T (2013). Adhesion in the stem cell niche: biological roles and regulation. Development 140, 255–265. [PubMed: 23250203]

23. Tian A, and Jiang J (2014). Intestinal epithelium-derived BMP controls stem cell self-renewal in *Drosophila* adult midgut. Elife 3, e01857. [PubMed: 24618900]

24. Conboy IM, and Rando TA (2002). The regulation of Notch signaling controls satellite cell activation and cell fate determination in postnatal myogenesis. Dev Cell 3, 397–409. [PubMed: 12361602]

25. Blanpain C, Lowry WE, Pasolli HA, and Fuchs E (2006). Canonical notch signaling functions as a commitment switch in the epidermal lineage. Genes Dev 20, 3022–3035. [PubMed: 17079689]

26. Brenner S (1974). The genetics of *Caenorhabditis elegans*. Genetics 77, 71–94. [PubMed: 4366476]

27. Merritt C, Rasoloson D, Ko D, and Seydoux G (2008). 3' UTRs are the primary regulators of gene expression in the *C. elegans* germline. Curr Biol 18, 1476–1482. [PubMed: 18818082]

28. Frokjaer-Jensen C, Davis MW, Hopkins CE, Newman BJ, Thummel JM, Olesen SP, Grunnet M, and Jorgensen EM (2008). Single-copy insertion of transgenes in *Caenorhabditis elegans*. Nat Genet 40, 1375–1383. [PubMed: 18953339]

29. Gibson DG, Young L, Chuang RY, Venter JC, Hutchison CA 3rd, and Smith HO (2009). Enzymatic assembly of DNA molecules up to several hundred kilobases. Nat Methods 6, 343–345. [PubMed: 19363495]

30. Wehman AM, Poggioli C, Schweinsberg P, Grant BD, and Nance J (2011). The P4-ATPase TAT-5 inhibits the budding of extracellular vesicles in *C. elegans* embryos. Curr Biol 21, 1951–1959. [PubMed: 22100064]

31. Nance J, Munro EM, and Priess JR (2003). *C. elegans* PAR-3 and PAR-6 are required for apicobasal asymmetries associated with cell adhesion and gastrulation. Development 130, 5339–5350. [PubMed: 13129846]

32. Mello CC, Kramer JM, Stinchcomb D, and Ambros V (1991). Efficient gene transfer in *C.elegans*: extrachromosomal maintenance and integration of transforming sequences. EMBO J 10, 3959–3970. [PubMed: 1935914]

33. Armenti ST, Lohmer LL, Sherwood DR, and Nance J (2014). Repurposing an endogenous degradation system for rapid and targeted depletion of *C. elegans* proteins. Development 141, 4640–4647. [PubMed: 25377555]

34. Kamath RS, Fraser AG, Dong Y, Poulin G, Durbin R, Gotta M, Kanapin A, Le Bot N, Moreno S, Sohrmann M, et al. (2003). Systematic functional analysis of the *Caenorhabditis elegans* genome using RNAi. Nature 421, 231–237. [PubMed: 12529635]

35. Anderson DC, Gill JS, Cinalli RM, and Nance J (2008). Polarization of the *C. elegans* embryo by RhoGAP-mediated exclusion of PAR-6 from cell contacts. Science 320, 1771–1774. [PubMed: 18583611]

36. Choi B, Kang J, Park YS, Lee J, and Cho NJ (2011). A possible role for FRM-1, a *C. elegans* FERM family protein, in embryonic development. Mol Cells 31, 455–459. [PubMed: 21448586]

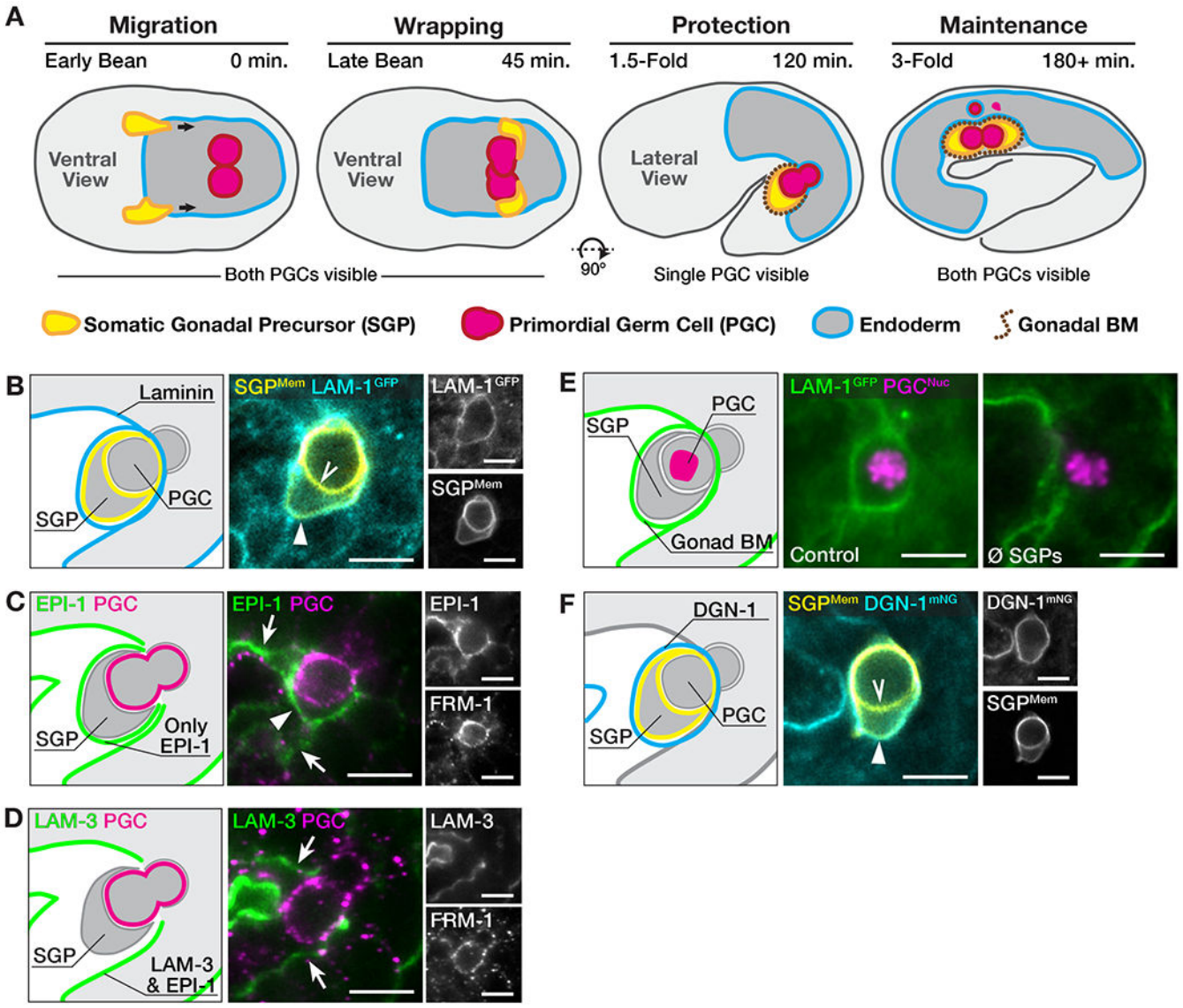

Figure 1. SGP wrapping templates the gonadal basement membrane

(**A**) Stages of gonad primordium formation. The embryo rotates onto its side between late-bean and 1.5-fold stages. (**B**) Localization of LAM-1^{GFP} to outward-facing (arrowhead) but not inward-facing (chevron) SGP surfaces. (**C-D**) Localization of EPI-1 and LAM-3. Arrowhead, gonadal BM; arrow, non-gonadal BM. FRM-1 marks membranes. (**E**) LAM-1^{GFP} in the gonad primordium of control and SGP-ablated (∅ SGPs) embryos. (**F**) DGN-1^{mNG} localization to the outward-facing (arrowhead) but not inward-facing (chevron) surfaces of the SGPs. Scale bars, 5μm. See Figure S1.

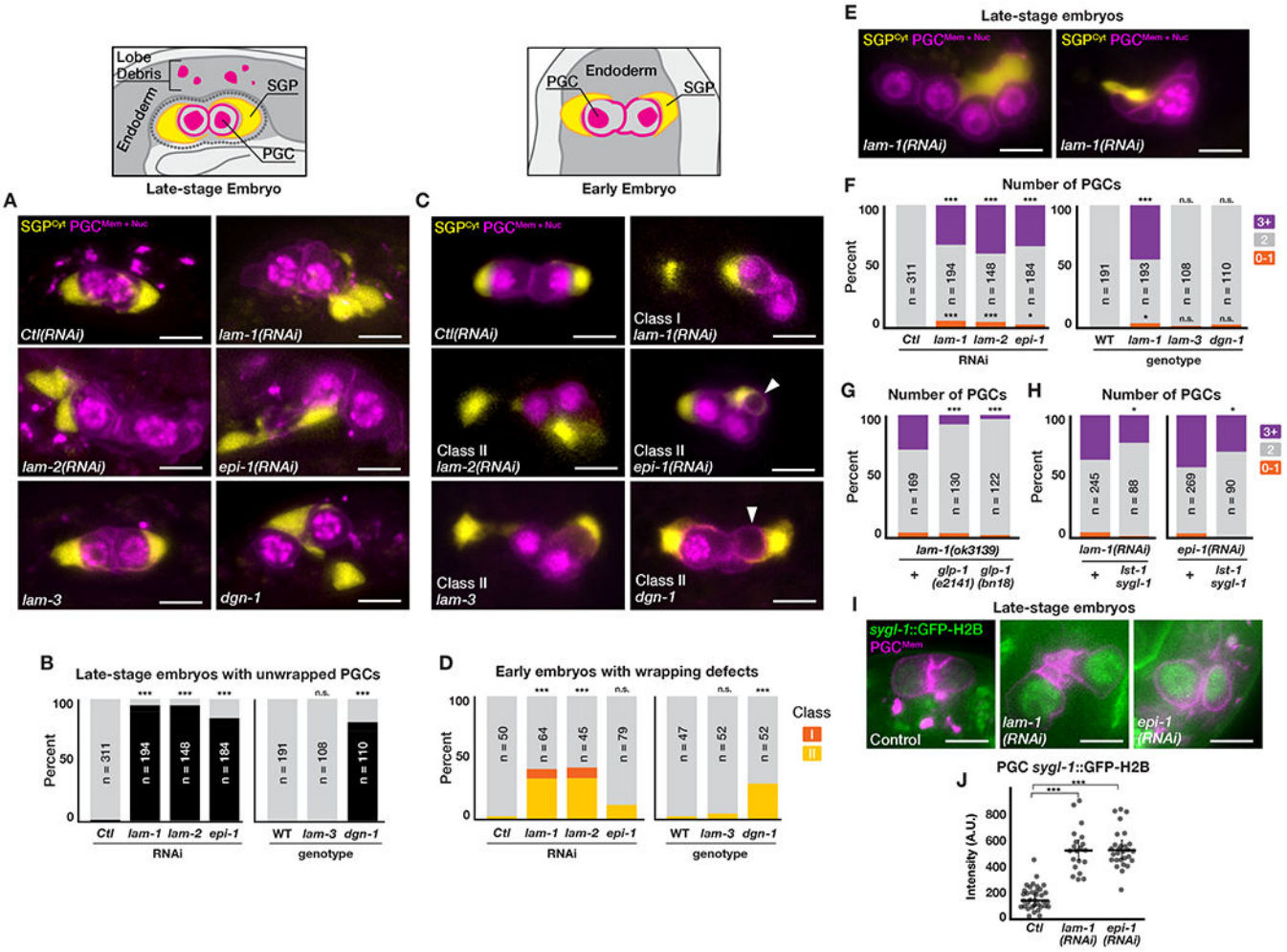

Figure 2. Basement membrane maintains SGP wrapping and GLP-1-regulated PGC quiescence

(A) SGP wrapping of PGCs in late-stage embryos. **(B)** Quantification of SGP wrapping defects in late-stage embryos. **(C)** SGP wrapping of PGCs in early embryos; arrowheads, SGPs wrapping PGC lobes. **(D)** Quantification of SGP wrapping defects in early embryos; see Results for phenotype Classes. **(E)** Extra (left) or reduced (right) PGC number in *lam-1(RNAi)* embryos. **(F)** Quantification of PGC number in late-stage embryos. **(G)** Suppression of extra PGCs in *lam-1* mutants by *glp-1*. **(H)** Partial suppression of extra PGCs in *lam-1(RNAi)* and *epi-1(RNAi)* embryos by *lst-1 sygl-1*. **(I)** *sygl-1*::GFP-H2B reporter in PGCs of the indicated genotype. **(J)** Quantification of *sygl-1*::GFP-H2B expression in PGCs. Bar is median and error bars are 95% C.I. (B,D,F–H) Fisher's exact test; (J) two-tailed t-test; ***$p \leq 0.001$, *$p \leq 0.05$, n.s. not significant. Scale bars, 5 μm. See Figures S2 and S3.

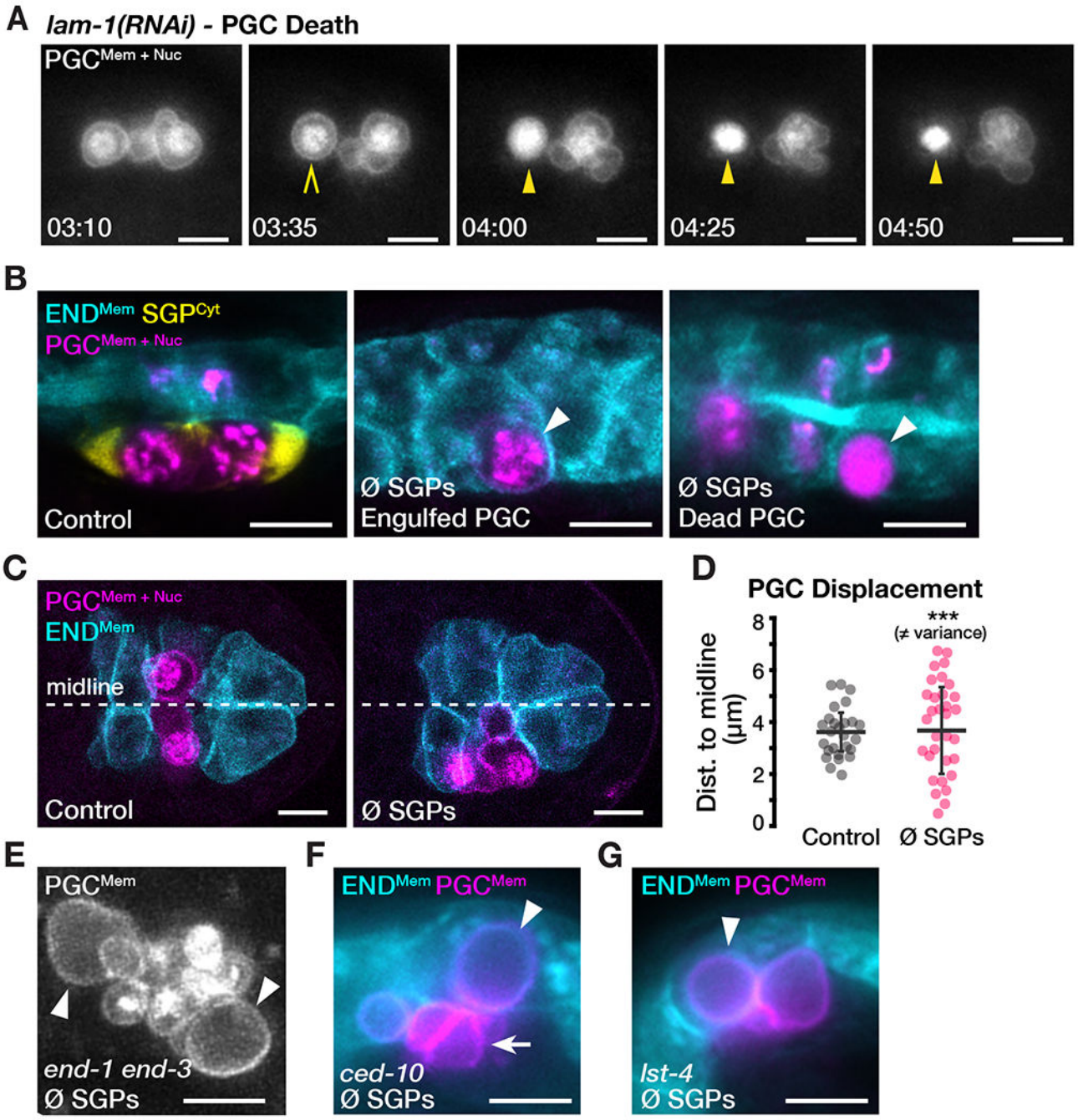

Figure 3. Unwrapped PGCs are cannibalized by endodermal cells

(A) Time-lapse sequence showing PGC death in a *lam-1(RNAi)* embryo (PGC before death, chevron; degrading PGC, arrowheads). Times are hours:min relative to gonad primordium formation. (**B**) Relative positions of SGPs, PGCs and endodermal cells in control and SGP-ablated (∅ SGPs) late-stage embryos. Arrowheads, engulfed (middle panel) or degrading (right panel) PGC cell body. **(C)** PGC position at the time of gonad assembly in control and SGP-ablated embryos. Dashed line, midline. **(D)** Analysis of variance in PGC position in control and SGP-ablated embryos, compared using an F-test for equality of variance

(***$p \leq 0.001$; control, n=26; SGP-ablated, n=35). Mean(bar) and S.D. are indicated. **(E)** *end-1 end-3* SGP-ablated embryo showing surviving PGC cell bodies (arrowheads) and persistent lobes. **(F-G)** PGC cell body (arrowhead, identified by DIC) inside of endodermal cells in *ced-10* and *lst-4* mutant SGP-ablated embryos. Arrow, unengulfed lobes. Scale bars, 5 μm. See Figure S4.

Table 1.

PGC loss after SGP ablation

Genotype	Perturbation or class	Number of PGCs				*n*	*p* value[b]
		Two PGCs	One PGC	No PGCs	% Death		
wild type	None	132	0	0	0%	132	
wild type	Control ablation	15	0	0	0%	15	1
wild type	Double SGP ablation	16	16	8	40%	40	<0.0001
wild type	Single SGP ablation	10	5	0	17 %	15	<0.0001
ced-3	Double SGP ablation	7	6	2	33 %	15	0.762
ced-10	Double SGP ablation	12	1	0	4%	13	0.0011
lst-4	Double SGP ablation	17	1	1	8%	19	0.0005
ehn-3 + Ctl(RNAi)	Two SGPs present	76	0	0	0%	76	
ehn-3 + hnd-1(RNAi)	Two SGPs present	57	2	0	2%	59	0.189
ehn-3 + hnd-l(RNAi)	One SGP present	62	29	1	17%	92	<0.0001
ehn-3 + hnd-l(RNAi)	No SGPs present	23	6	0	10%	29	0.0003
end-1 end-3 rescued[a]	Double SGP ablation	5	7	6	53 %	18	
end-1 end-3	Double SGP ablation	17	1	0	3 %	18	0.0001
Ctl(RNAi)	Double SGP ablation	5	6	4	47%	15	
lam-1(RNAi)	Double SGP ablation	6	4	2	34%	12	0.452
lam-2(RNAi)	Double SGP ablation	3	8	1	42%	12	0.696

[a] *end-1(ok558) end-3(ok1448)* rescued with *irEx568 [end-1(+), end-3(+), sur-5::dsRed]*

[b] *p* values were calculated using Fisher's Exact Test, comparing between samples the fraction of embryos with fewer than two PGCs. Ablations performed in a wild-type background were compared with unperturbed WT embryos. Ablations in *ced-3, ced-10* and *lst-4* embryos were compared with ablated wild-type embryos, *ehn-3 + hnd-1(RNAi)* embryos were compared with *ehn-3 + Ctl(RNAi)* embryos. Ablated *end-1 end-3* embryos were compared with rescued ablated *end-1 end-3* embryos. Ablated *lam-1(RNAi)* and *lam-2(RNAi)* embryos were compared with ablated *Ctl(RNAi)* embryos.

Key Resource Table

REAGENT or RESOURCE	SOURCE	IDENTIFIER
Antibodies		
Chicken anti-EPI-1	Wadsworth Lab [5]	N/A
Chicken anti-LAM-3	Wadsworth Lab [5]	N/A
Mouse anti-FRM-1	Cho Lab [36]	N/A
Alexa 647 donkey anti-chicken IgY	Jackson ImmunoResearch	Cat# 703-606-155
Alexa 488 goat anti-mouse IgG	Thermo Fisher Scientific	Cat# A28175
Bacterial and Virus Strains		
E. coli RNAi feeding strain	*Caenorhabditis* Genetics Center	HT115
E.coli OP50	*Caenorhabditis* Genetics Center	OP50
Biological Samples		
Chemicals, Peptides, and Recombinant Proteins		
Trioxsalen	Sigma	Cat# T6137
7-Amino-4-Methylcoumarin	Sigma	Cat# 257370
Critical Commercial Assays		
Deposited Data		
Experimental Models: Cell Lines		
Experimental Models: Organisms/Strains		
ced-10(n1993); xnls360 [mex-5p::mCherry-PH$_{PLC1\delta1}$::nos-2 3'UTR, unc-119(+)]; zuls70 [end-1p::GFP-CAAX, unc-119(+)]	[4]	FT1214
lst-4(xn45); xnls360; zuls70; lin-2(e1309)	[4]	FT1468
end1(ok558) end3(ok1448) xnls360; irEx568 [end-1(+), end-3(+), sur-5::RFP]; xnls525 [ehp-3p::YFP, unc-119(+)]; xnEx295 [end-1p::CFP-CAAX, unc-119(+)]	This study	FT1701
xnls360; naSi2 [mex-5p::mCherry-H2B::nos-2 3'UTR]; xnls525; xnEx295	This study	FT1703
ehn-3(q689); xnls360; naSi2; xnls525	This study	FT1718
naSi2; qyls10 [lam-1p::lam-1-GFP, unc-119(+)]	This study	FT1936
ced-3(n717); naSi2; glh-1(xn82 [glh-1p::mCardinal-PH::glh-1 3'utr])	This study	FT1939
dgn-1(qy18 [dgn-1 ::mNeonGreen]); naSi2	This study	FT1975
dgn-1(cg121); cgEx308 [dgn-1(+), dgn-1p::dgn-1-GFP, rol-6(su1006)]; xnls360; naSi2; xnls525; xnEx295	This study	FT1983
xnls510 [ehn3p::mCherry-PH, unc-119(+)]; qyls10	This study	FT2014
dgn-1(qy18 [dgn-1::mNeonGreen]); xnls510	This study	FT2046
lam-3(ok2030)/tmC18 [dpy-5(tmls1200)]; xnls360; naSi2; xnls525	This study	FT2052
akt-1(ok525); naSi2	This study	FT2075
lst-1(ok814) sygl-1(tm5040)/tmC27 [unc-75(tmls1239)];naSi2	This study	FT2160

REAGENT or RESOURCE	SOURCE	IDENTIFIER
lam-1(ok3139); glp-1(e2141ts); naSi2; zuEx288 [lam-1(+), SUR-5::GFP]	This study	FT2163
lam-1(ok3139); naSi2; zuEx288	This study	FT2169
lam-1(ok3139); glp-1(bn18ts); naSi2; zuEx288	This study	FT2176
Oligonucleotides		
lam-1(RNAi) For: 5'–GTGCCGACATTACTCATTACG–3'	This study	N/A
lam-1(RNAi) Rev: 5'–CTCCGAGTCTTGGATCTC–3'	This study	N/A
lam-2(RNAi) For: 5'–CCCAAGAATCAATGAACTCGAA–3'	This study	N/A
lam-2(RNAi) Rev: 5'–CATCCATTGGCACTGAATCC–3'	This study	N/A
hnd-1(RNAi) For: 5'–CTGGAAACAATGCGGTTTCT–3'	This study	N/A
hnd-1(RNAi) Rev: 5'–CCGGAAACGGACTTTACAAT–3'	This study	N/A
Recombinant DNA		
epi-1 feeding RNAi clone	Ahringer RNAi library [30]	clone K08C7.3
lam-1 feeding RNAi clone	This study	PDCM101
lam-2 feeding RNAi clone	This study	PDCM102
hnd-1 feeding RNAi clone	This study	pDCM103
Expression vector with *ehn-3p::mCherry-PH*$_{PLC1\partial1}$	This study	pYA12
Expression vector with *ehn-3p::YFP*	This study	pDCM03
Expression vector with *end-1p::CFP-CAAX*	This study	pJN585
Software and Algorithms		
FIJI v2.0	FIJI	https://fiji.sc/
Zeiss Zen software v2.0	Carl Zeiss	https://www.zeiss.com/microscopy/us/products/microscope-software/zen.html
Adobe Photoshop CC v19.0	Adobe Systems	https://www.adobe.com/products/photoshop.html
Other		